



(RESEARCH ARTICLE)



Evaluation of dry sliding wear characteristics of hybrid a356 composite

Mudashiru Lateef Owolabi ¹, Babatunde Issa Akinola ¹, Adewale Taiwo Olasumboye ², Adetola Sunday Olufemi ^{1,*} and Oyejide Ayodele James ¹

¹ Department Mechanical Engineering, Ladoké Akintola University of Technology, Ogbomoshó, Nigeria.

² Corning Research and Development Corporation, Corning Incorporated, Corning NY 14830.

International Journal of Science and Research Archive, 2024, 12(02), 2458–2466

Publication history: Received on 05 July 2024; revised on 20 August 2024; accepted on 23 August 2024

Article DOI: <https://doi.org/10.30574/ijrsra.2024.12.2.1495>

Abstract

As advancements in lightweight and synthetic materials have evolved, our ability to tailor materials to meet societal demands has expanded. Aluminium alloys, known for their high strength-to-weight ratio and cost-effectiveness, are extensively utilized in engineering applications, including structural casting and automotive components. This study employed the stir casting method to investigate the impact of silicon carbide (SiC) and graphite (Gr) on a hybrid A356 composite, aiming to enhance its tribological applicability. SiC and Gr particles were processed using a vibratory ball milling machine for two hours, followed by composite fabrication with varying particle sizes. Microstructural investigation using optical microscopy revealed maximum hardness values of 127 BHN and 125 BHN for A356 composites reinforced with 12.50% SiC, 15.50% Gr, and 11.43% SiC, 15.86% Gr, respectively. Wear rate analysis demonstrated that reinforced A356 composites exhibited higher wear resistance compared to unreinforced alloys. Notably, the sample reinforced with 11.43% SiC and 15.86% Gr displayed exceptional wear resistance. Photo micrographs of A356-SiC-Gr samples at different sliding distances, velocities, and loads revealed minimal plastic deformation during wear testing, resulting in abrasive and cohesive wear. Overall, this study underscores the effectiveness of graphite (Gr) and silicon carbide (SiC) as reinforcement materials for enhancing the tribological properties of A356 composites.

Keywords: Characterization; Composite materials; Impact; Materials; Mechanical properties of material.

1. Introduction

The advancement of lightweight materials has revolutionized the capability to engineer materials to meet evolving societal demands [1-3]. Cast alloy materials like aluminium, magnesium, and titanium alloys have become prevalent for mass production, finding widespread applications across various industries [4-5]. Additionally, composite lightweight materials have emerged as a focal point in engineering applications, offering tailored properties to meet specific requirements [6]. In applications where a high strength-to-weight (STW) ratio and favorable tribological properties are essential, the A356 alloy is frequently employed. This alloy finds extensive use in automotive components, pump housings, high-velocity blowers, and structural castings [2]. Notably, A356 and similar low-iron concentration Al-alloys like A380 and A319 offer the optimal combination of strength and ductility for moderately loaded cylinder heads of gasoline engines [3, 6].

Engine component manufacturing poses significant challenges in cost-effectiveness for automotive designers. To address this, cast alloys based on aluminium often replace grey cast iron cylinder blocks and other engine components. In the A356 alloy, primary particles are primarily in the α -phase at the end of solidification, with eutectic filling the interstitial spaces [7-12]. The morphology of the eutectic, crucial for mechanical properties, is influenced by the size and shape of segregated silicon particles. Incorporating a second reinforcing phase, such as graphite, silicon carbide, or

* Corresponding author: Adetola Sunday Olufemi

nitride particles, further enhances the appeal of these alloys [9]. However, the use of composite materials in engine tribology is susceptible to damage due to the presence of silicon phases, particularly at low strains. Hence, literature suggests incorporating micro-additions of reinforcing materials like SiC or Gr, or their combinations, to enhance mechanical qualities [13]. Various processing methods, including squeeze casting, infiltration, powder metallurgy, and stir casting, can produce metal matrix composites (MMCs). Stir casting, especially effective for up to 30% volume reinforcement, faces challenges related to the separation and settling of reinforcing particles during melting and casting [8, 14]. Achieving a homogeneous distribution of reinforcements within the matrix is critical for reducing porosity levels, refining microstructure, and enhancing mechanical properties [15]. Therefore, this study aims to evaluate the hardness and wear properties of SiC and Gr reinforcements of varying sizes (60, 53, 44, 37, and 26 μm) in an A356 aluminium matrix.

2. Materials and methods

2.1. Matrix Material and Reinforcement

2.1.1. Aluminium A356

For this study, the commercial aluminium alloy A356 was employed, characterized by silicon and magnesium as its primary alloying constituents. Table 1 outlines the composition details of A356. Renowned for its exceptional castability, high strength, and elongation properties, this alloy is well-suited for thin parts and applications demanding pressure resistance. A356 stands out as the most widely used aluminium alloy, finding diverse applications across various industries [5-7].

2.1.2. Silicon Carbide (SiC)

Renowned for its durability and affordability in demanding environments, silicon carbide (SiC) stands as a favored abrasive and modern engraving material. Composed of silicon and carbon, SiC, also known as carborundum, is highly versatile. By sintering Si-C particle grains, exceptionally hard ceramics are formed, extensively employed in applications such as brake pads, aerospace components, and military equipment. The addition of SiC to aluminum matrix composites has been shown to enhance tensile strength and hardness, offering promising reinforcement capabilities [11].

Table 1 Chemical Composition of A356 Alloy

Elements	(wt.%)
SiC	7.25
Fe	0.47
Mn	0.26
Zn	0.31
Cu	0.24
Ti	0.17
Mg	0.28
Al	Bal.

2.1.3. Graphite (Gr)

Graphite consists of tightly interconnected carbon atom sheets, characterized by weakened shear strength due to the inherently weak bonds between these sheets. This attribute has established graphite as a fundamental solid lubricating material owing to its strength and hardness [2,15]. Table 2 delineates the properties of SiC and Gr for reference.

Table 2 Physical properties of Silicon Carbide and Graphite

Reinforcement	SiC	Gr
Young Modulus (GPa)	8 - 15	4.1
Density (g/cm ³)	2.26	1.61
Hardness (VHN)	92	235
Poisson ratio	0.31	0.17
Crystal Structure	Covalent Hexagonal	

2.2. Stir Casting Process

Stir casting emerges as a cost-effective and straightforward method for fabricating metal matrix composites, offering precise control over composite structure modification [16-17]. This casting process involves introducing a mechanical stirrer into the molten metal to create a vortex, facilitating the mixing of reinforcement with the matrix [18]. As depicted in Figure 1a, an impeller blade generates the vortex, enabling the incorporation of reinforcement material into the melt. The impeller blade, connected to variable speed motors via a shaft, rotates at controlled speeds to facilitate mixing. Reinforcement powders, both SiC and Gr, underwent grinding in a vibratory ball milling machine to ensure homogeneity. The milling process lasted 2 hours, employing a ball/powder ratio of 6/1 by weight, a ball diameter of 20 mm, and a speed of 250 rpm [6]. Following milling, the reinforcement powders were sieved to obtain particle sizes of 60, 53, 44, 37, and 26 μm , adhering to ASTM E-11 standards.

During experimentation, the matrix material underwent melting in an electric furnace, maintained at 750 °C for 3 minutes. Simultaneously, reinforcements were preheated in a separate crucible to enhance wettability before introduction into the melt. Notably, the molten metal was shielded from oxidation using white sodium tetraborate pentahydrate before reinforcement addition. Following reinforcement introduction, vigorous stirring with a mechanical stirrer ensued for 2 minutes to ensure a homogeneous mixture. The resulting melt was poured into a sand mold measuring 200 by 200 by 100 mm. Subsequently, composite test specimens with dimensions $\text{\O}10$ mm by 150 mm length were cast, as illustrated in Figure 1b.

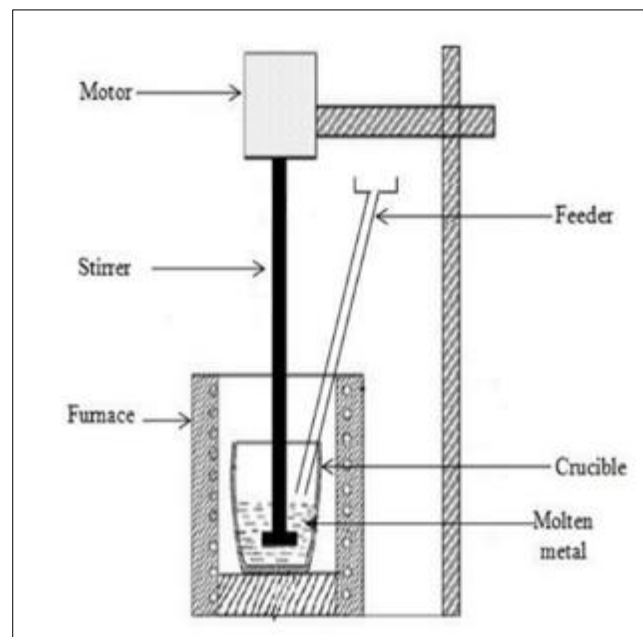
**Figure 1a** Schematic of stir casting setup



Figure 1b Cast samples

2.3. Material Characterization

The composite samples, both unreinforced and reinforced, underwent grinding, polishing, and etching following standard metallographic surface preparation procedures for microstructure analysis. Understanding the microstructure of cast specimens is crucial for assessing material structure and performance in service, encompassing factors such as size, shape, phase/particle distribution, and the presence of defects [19-20]. Prior to analysis, samples underwent grinding with progressively finer-grade emery papers (22, 32, 40, and 60 μm) in accordance with ASTM E3 standards, transitioning from coarse to fine grades. Polishing was conducted under running water to remove grit and prevent overheating, utilizing emery cloths soaked in a 0.5 μm silicon carbide solution until achieving a mirror-like surface.

Etching of the materials occurred in a 2% sodium hydroxide solution (NaOH) for 5 to 10 seconds to reveal the internal structure. Subsequently, the samples were washed, dried, and observed under an inverted Leica DMi8 optical metallurgical microscope.

2.4. Mechanical Properties

The mechanical properties of the material determined include wear rate, hardness compressive and impact strengths.

2.4.1. The sliding wear

The characteristics of the unreinforced alloy (0 wt.%) and the composites reinforced with different amount of SiC and Gr mixtures (wt.%) were studied at room temperature utilizing pin-on-disc machine (Fig. 2) in dry condition. The cylindrical test pins 40 mm and diameter of 5 mm were machined from the cast specimen. The samples were mounted perpendicularly on a rotating disc and were driven against a steel counterpart that was fixed on a lever mechanism with an applied load of 20 kg. The wear rates were studied as a function of sliding velocity and distance. The steady state wear rate was calculated using the relation:

$$W = M/\rho D \quad (1)$$

where W is the steady state wear rate (mm^3/m), M is the mass loss (g), ρ is the density (g/mm^3) and D is the sliding distance in (m)



Figure 2 The pin-on disc wear testing

2.4.2. Hardness and Compression Test

The Brinell hardness tests were done according to ASTM-E10-95 and for compression test following the ASTM-E9-95 standard. Specimens of 10 mm diameter were thoroughly cleaned in Machine. various emery papers and the tests were conducted in three distinct areas on the hardness round specimens both for unreinforced and reinforced A356 composites

2.4.3. Determination of impact strength

Impact tests were conducted using a fully instrumented Avery Denison™ test machine. The machine can provide a range of impact energies from 0 to 300 J. The mass of the hammer was 22.7 kg and the striking velocity 3.5 m/s. Charpy impact tests were conducted on notched specimens. Standard square impact test specimen measured 50 mm × 10 mm × 10 mm with notch depth of 2 mm and a notch tip radius of 0.02 mm at angle of 45° was used for this research.

3. Result and discussion

The weight percentage variation of A359 alloy, SiC and Gr for the preparation of the specimen are given in Table 3.

Table 3 Percentage compositions of the hybrid metal matrix composites (wt.%)

Samples	Weight % variation of A356 and reinforcements
Control	A356 (unreinforced)
A	72.56% + 17.39% SiC + 10.05% Gr
B	71.54% + 15.38% SiC + 13.08% Gr
C	75.17% + 13.79% SiC + 11.04% Gr
D	72.00% + 12.50% SiC + 15.50% Gr
E	72.71% + 11.43% SiC + 15.86% Gr

3.1. Wear Rate

The study investigated the wear rate under different sliding distances at a 20 kg load, correlating it with hardness, as depicted in Figures 3(a) and (b). The sliding velocity ranged from 1 m/s to 2.5 m/s [21]. Figure 3(a) illustrates the wear rate at a sliding distance of 1000 m with a velocity of 1 m/s, while Figure 3(b) illustrates the wear rate at a sliding

distance of 2500 m with a velocity of 2.5 m/s. Notably, samples E and F exhibited the least wear rate at higher sliding distances and velocities, indicative of the effective interfacial bonding between the reinforcements and the matrix material.

3.2. Compression and Impact Strength

Table 4 presents the compression strength results derived from the compression tests conducted on the prepared composites. As the weight percentage of the SiC and Gr mixture reinforcement increased, so did the compression strength of the composites. This enhancement in compression strength is attributed to direct reinforcement, facilitating the transfer of load from the A356 matrix to the reinforcement material. The highest compressive strength was achieved with the A356-13.79%SiC-11.04%Gr composition, indicating robust bonding between the reinforcement and the matrix. Similarly, Table 4 also illustrates the impact energy results, which increased with the percentage addition of the SiC-Gr mixture. The reinforced material significantly contributed to enhancing the impact strength of the composite, with the highest impact energies observed in samples E and F. This suggests greater material toughness, particularly with a higher Gr content in the composite.

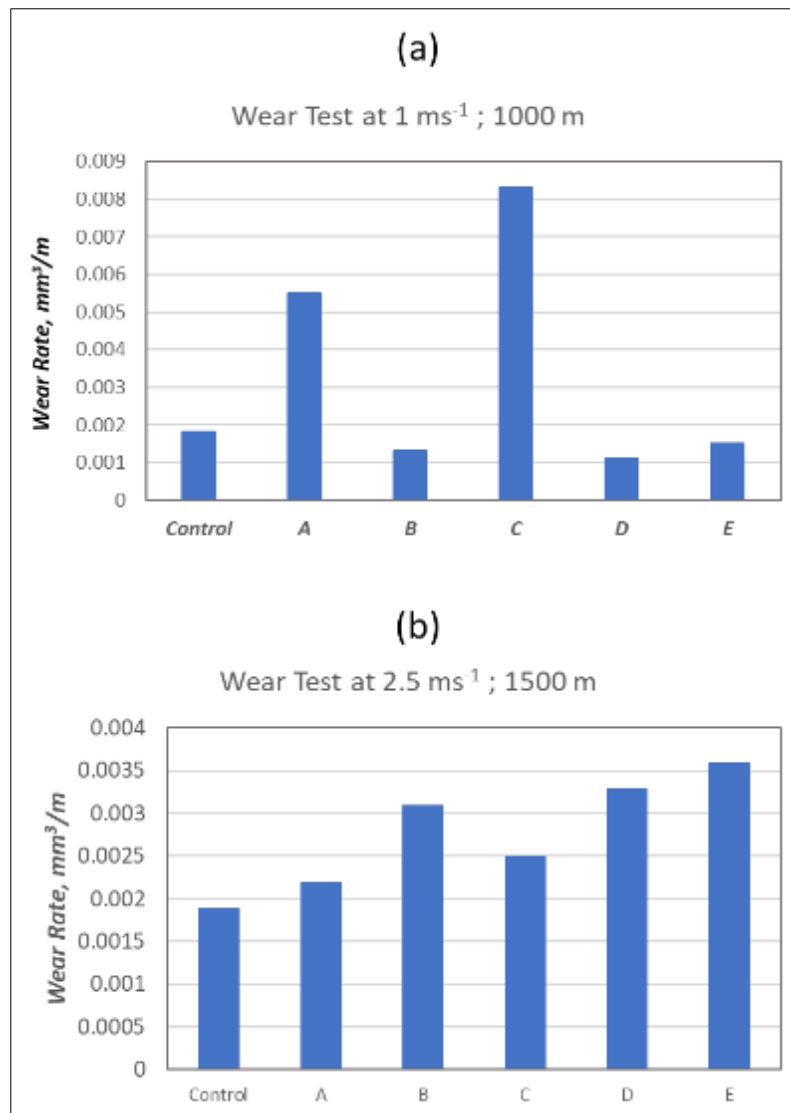


Figure 3 Wear rate at (a) 1-ms-1 velocity and 1000-m sliding distance; and (b) 2.5-ms-1 velocity and 1500-m sliding distance

Table 4 Compression and impact strength values of the prepared composites

SPECIMEN	CS(MPa)	IS (J)
A356 Reference	457	16
Sample B	463	21
Sample C	492	21
Sample D	489	22
Sample E	494	21
Sample F	498	23

3.3. Microstructural Analysis

The process of examining materials at a sub-micron scale to ascertain details ranging from the straightforward assessment of grain size to the comprehensive characterization of multi-component systems is known as microstructural analysis [22, 23]. Figure 4 displays the photomicrographs of A356 and A356-SiC-Gr materials under varying sliding distances, velocities, and loads. In Figures 4(b-e), minimal plastic deformation of asperities is evident during the wear test, resulting in abrasive and cohesive wear. The composite exhibits reduced material removal and fewer cracks on the worn surface compared to A356 alone. With increasing sliding distance, material loss becomes more pronounced, expanding in the sliding direction and leaving no shell holes in the material. Both SiC and Gr reinforcement particles demonstrate favorable bonding characteristics.

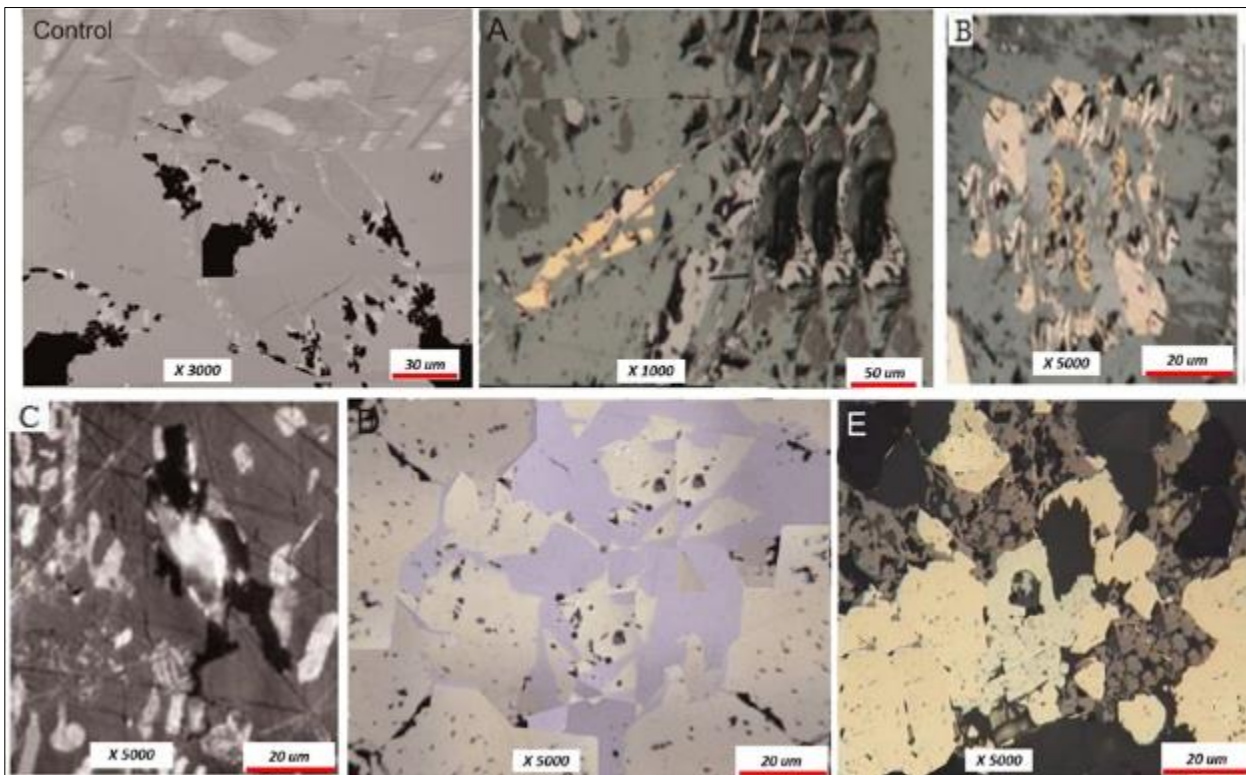


Figure 4 Optical Micrographs of worm pin-on-disc Tensile Characteristics of Al 356 alloy reinforced surface of A356-SiC-Gr at load 10kg for different velocities and sliding distances: (a) 1 m/s and 1000 m (b) Composite. Procedia Engineering 97, 614 – 624, 1 m/s and 1500 m, (c) 1.5 m/s and 1500 m, (d) 2 m/s and 1500 m, (e) 2.5 m/s and 1000 m

4. Conclusions

The study examined the impact of SiC and Gr reinforcements on the wear properties of A356 cast aluminum alloy. Impact strength and wear properties of the modified alloy were evaluated and compared with those of the control material. The investigation of wear rate for the A356-SiC-Gr composite concerning sliding velocity and distance revealed

notable wear behavior at a lower velocity of 1 m/s in samples A and C, where the ratio of Gr to the base alloy content was lower. Conversely, wear rate significantly decreased at higher Gr to base alloy ratios in samples B, D, and E, suggesting Gr's role as a wear-limiting agent. At a higher velocity of 1.5 m/s, wear rate generally increased across the sample range from the control material to sample E. The findings indicate that the composites are suitable primarily for low-speed applications where minimal wear is desirable. Consequently, the addition of graphite in the matrix acts as a lubricant, enhancing the material's wear resistance.

Compliance with ethical standards

Acknowledgments

The authors of this research would like to thank Dr. Aloo, Dr. Aminu and Prof. Adeyi for their valuable technical assistance. We are also grateful for partial support from Group Engineer, Material Lab, Kwara State University, Molete, Nigeria, for making use of their equipment.

Disclosure of conflict of interest

No conflict of interest to be disclosed.

References

- [1] J. Campbell, "Materials Perspective, Entrainment Defects," *Material Science Technology*, vol. 22, no. 2, pp. 132–136, 2006.
- [2] F. P. Bowden and D. Tabor, *The Friction and Lubrication of Solids, Part II*, Oxford University Press, UK, pp. 320–331, 1964.
- [3] S. Das, "The cost of automotive polymer composites: A review and assessment of DOE's lightweight materials composites research," *ORNL-TM*, pp. 283–291, 2000.
- [4] A. J. Oyejide, S. O. Adetola, and A. Lawal, "Machine design approach to bone waste utilization in slaughterhouses of developing countries with focus on Nigeria," *World Journal of Engineering and Technology*, vol. 10, no. 2, pp. 444–457, 2022.
- [5] Adetola, S.O. and Oyejide, A.J., 2015. Development of a bone milling machine with safety hollow and low risk of electrical damage. *International Journal of Modern Engineering Research*, 5(6), pp.52-59.
- [6] J. R. Davis, ed., *Aluminum and Aluminum Alloys*, ASM Specialty Handbook, ASM International, pp. 312–344, 1993.
- [7] B. P. Dileep and B. R. Sridhar, "An Investigation on Mechanical and Metallurgical Properties of Steel EN24 and SiC MMCs," *International Journal of Mechanical and Production Engineering Research and Development*, vol. 8, no. 2, pp. 189–194, 2018.
- [8] B. Geetha and K. Ganesan, "Optimization of Journal of Material Science," vol. 48, pp. 4365–4377, 2013.
- [9] J. Hashim, L. Looney, and M. S. J. Hashmi, "Metal Matrix Composites: Production by the Stir Casting Method," *Journal of Materials Processing Technology*, vol. 119, no. 1-3, pp. 329–335, 1999.
- [10] R. Karunanithi, S. Bera, and K. Ghosh, "Electrochemical behaviour of TiO₂ reinforced Al 7075 composite," *Materials Science and Engineering: B*, vol. 190, pp. 133–143, 2014.
- [11] M. Ravikumar, H. N. Reddappa, and R. Suresh, "Aluminum Composites Fabrication Technique and Effect of Improvement in Their Mechanical Properties - A Review," *Materials Today Proceedings*, vol. 5, no. 11, pp. 23796–23805, 2018.
- [12] M. T. Sijo and K. R. Jayadevan, "Analysis of Stir Cast Aluminum Silicon Carbide Metal Matrix Composite: A Comprehensive Review," *Procedia Technology*, vol. 24, pp. 379–385, 2018.
- [13] M. Singla, D. D. Dwivedi, L. Singh, and C. Vikas, "Development of Aluminum Based Silicon Carbide Particulate Metal Matrix Composite," *Journal of Minerals, Materials Characterization and Engineering*, vol. 8, no. 6, pp. 455–467, 2009.
- [14] Q. Shen, C. Wu, G. Luo, P. Fang, C. Li, Y. Wang, and L. Zhang, "Microstructure and mechanical properties of Al-7075/B4C composites fabricated by plasma activated sintering," *Journal of Alloys and Compounds*, vol. 588, pp. 265–270, 2014.

- [15] M. K. Surappa, "Aluminium matrix composites: Challenges and Opportunities," *Journal of Material Science*, vol. 28, no. 1–2, pp. 319–334, 2003.
- [16] T. Thirumalai, R. Subramanian, S. Kumaran, S. Dharmalingam, and S. S. Ramakrishnan, "Production and Characterization of Hybrid Aluminum Matrix Composites Reinforced with B4C and Graphite," *Journal of Scientific and Industrial Research*, vol. 73, pp. 667–670, 2014.
- [17] D. S. Thompson, B. S. Subramanya, and S. A. Levy, "Quench rate effects in Aluminum-Zinc-Magnesium-Copper alloys," *Journal of Metallurgical Transactions*, pp. 1149–1160, 1971.
- [18] L. Tomaz, "The structure and mechanical properties of Al-7%SiMg alloy treated with a homogeneous modifier," *Solid State Phenomena*, vol. 16, no. 21, pp. 183–186, 2010.
- [19] C. Zhang, X. He, Q. Liu, S. Ren, and Z. Qu, "Fabrication and Thermo-Physical Properties of Graphite Flake/Copper Composites," *Journal of Composite Materials*, vol. 214, pp. 214–217, 2020.
- [20] O. E. Joy, O. O. Abel, J. O. James, A. E. Oluwatosin, and O. Oyebola, "Preliminary Evaluation of Aluminium-Rice Husk Ash Composite for Prophylactic Knee Brace Production," *Composite Materials*, vol. 6, no. 1, pp. 32–38, 2022.
- [21] S. O. Adetola, A. J. Oyejide, E. O. Olayiwola, W. M. Ojekale, E. O. Joshua, and O. A. Busayo, "Effect of guinea-corn husk and saw-dust ash on the mechanical and microstructural properties of interlocking concrete block," *World Journal of Advanced Engineering Technology and Sciences*, vol. 12, no. 2, pp. 424–434, 2024.
- [22] S. Adetola, A. Oyejide, E. Emmanuel, S. Adejinle, and J. Aiyegbabe, "Microstructural Analysis of blended Guinea-Corn Stalk and Saw-Dust Ash for Cement Mixture of Interlocking Concrete Block," in *2024 International Conference on Science, Engineering and Business for Driving Sustainable Development Goals (SEB4SDG)*, IEEE, pp. 1–6, 2024.
- [23] S. O. Adetola, A. J. Oyejide, U. A. Olatunde, L. A. Isaac, and A. K. James, "Effect of particles size variation of graphite on mechanical properties of piston materials," *World Journal of Advanced Engineering Technology and Sciences*, vol. 12, no. 2, pp. 424–434, 2024.